

Philippe Jodin

APPLICATION OF NUMERICAL METHODS TO MIXED MODES FRACTURE MECHANICS EXPERIMENTS

PRIMENA NUMERIČKIH METODA U EKSPERIMENTIMA MEHANIKE LOMA SA MEŠOVITIM OBLIKOM LOMA

Original scientific paper
UDC: 539.42:519.6
Paper received: 31.01.2011

Author's address:
LABPS – Université Paul Verlaine – Metz et ENIM, Metz,
France

Keywords

- mixed modes fracture
- finite elements
- intrinsic curve

Ključne reči

- mešoviti oblik loma
- konačni elementi
- unutrašnje krive

Abstract

Several mixed mode fracture mechanics experiments are realized by the author before the year 1984. Several types of specimens are used: Centered Cracked Tensile sheets (CCT), Compact Mixed Mode (CMM), Compact Shear Specimen (CSS), unsymmetrical loading Single Edge Notch Bending three-points (ULSENB-3), and four-points (ULSENB-4). Computations of mode I K_I and mode II K_{II} stress intensity factors are made using calibration functions found in the literature, if any.

Results are presented in terms of intrinsic curves K_{II}/K_{Ic} versus K_I/K_{Ic} . However, some uncertainties remain about these calculated values. As today we have available much more efficient computers and software, additional finite elements computing is done on two kinds of specimens (CCT and ULSENB-3) and exact representation of some intrinsic curves are drawn.

As an example, the Mandel's criterion is computed and intrinsic curves for it are drawn. It is shown that concordance between criterion and computing results depends on the kind of behaviour law included in the software.

INTRODUCTION

In 1984, the author published an extensive study about mixed mode fracture, [2]. This work was based on extensive mixed modes fracture experiments. There was also a general review of various mixed modes fracture criteria. Up to 32 criteria for fracture and/or crack bifurcation have been noticed at this time. Most of them concern the elastic behaviour, but few the elasto-plastic one. However, when the proportion of mode II at the crack tip is important, failure occurs in an elastic-plastic way, and elastic analysis failed. At the time, powerful computing tools were not available for the author and rough behaviour estimations

Izvod

Nekoliko eksperimenata mehanike loma sa mešovitim oblikom loma su izvedeni od strane autora pre 1984. godine. Upotrebjeno je nekoliko tipova epruveta: zatezne trake sa središnjom prslinom (CCT), kompaktne epruvete za mešoviti lom (CMM), kompaktne epruvete za smicanje (CSS), epruvete za nesimetrično opterećenje sa jednostranim ivičnim zarezom i savijanjem u tri tačke (ULSENB-3) i u četiri tačke (ULSENB-4). Izračunavanje faktora intenziteta napona za tip loma I K_I i tipa loma II K_{II} je obavljeno korišćenjem kalibracionih funkcija iz literature, ako ih ima.

Rezultati su predstavljeni u vidu unutrašnjih krivih K_{II}/K_{Ic} prema K_I/K_{Ic} . Međutim, neke nesigurnosti ostaju oko ovih izračunatih veličina. Kako danas postoje mnogo efikasniji računari i softver, obavljeno je dopunsko računanje konačnim elementima na dve vrste epruveta (CCT i ULSENB-3) i dat je tačan prikaz nekih unutrašnjih krivih.

Kao primer, izveden je proračun prema kriterijumu Mandela i iscrtane su unutrašnje krive. Pokazuje se da poklapanje kriterijuma i proračunatih veličina zavisi od vrste zakona ponašanja koji je uključen u softver.

were done. Finally, a two-criteria analysis was proposed, where the behaviour of the structure was considered as either fully plastic, or fully elastic. Practically, limit state analysis or linear elastic fracture mechanics were applied.

The purpose of this work is to refine this analysis, using modern computer finite elements methods and general computing software. As an example, only the case of central cracked tensile (CCT) (Fig. 1) and asymmetrical three-points single edge notch bending (ULSENB-3) (Fig. 2) specimens will be analysed.

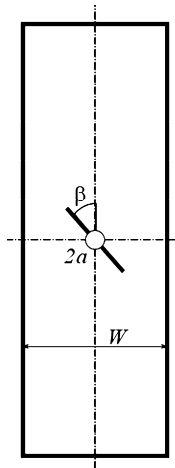


Figure 1. The CCT specimen.
Slika 1. CCT epruveta.

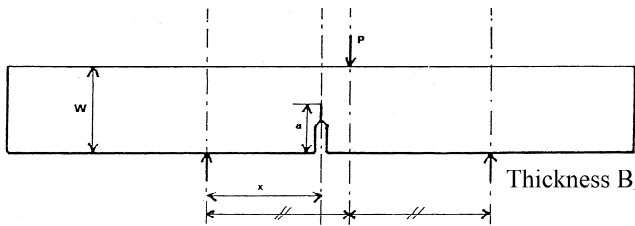


Figure 2. Asymmetrical three-points single edge notch bending specimen.

Slika 2. Nesimetrična epruveta sa zarezom za savijanje u tri tačke.

MIXED MODE FRACTURE CRITERIA

Elastic analysis

A bibliographical survey shows that the search for a valid linear elastic fracture criterion is always of interest. Most of papers analyse both the fracture and the bifurcation angle criterion. Results are generally presented in terms of a so-called "intrinsic curve" K_{II}/K_{Ic} vs. K_I/K_{Ic} . Such a curve is presented in Fig. 3.

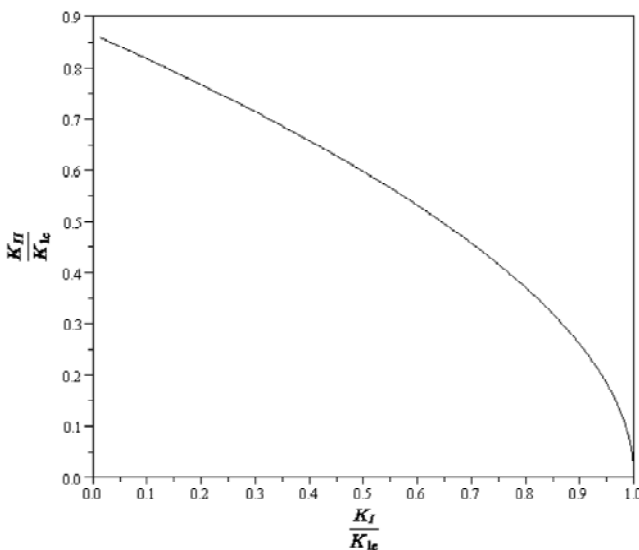


Figure 3. A typical intrinsic curve.
Slika 3. Tipična unutrašnja kriva.

Similarly, the bifurcation angle θ_0 is generally presented as θ_0 vs β , where β is the angle computed from

$$\beta = \arctan \frac{K_I}{K_{II}} \quad (1)$$

by reference to the CCT specimen, where β is the angle made by the crack with the loading axis (Fig. 1).

In several papers, the θ_0 angle is computed from the criterion of the maximum tangential stress (the MTS criterion) proposed by Sih, /1/. This criterion postulates that:

1. fracture occurs from the initial crack tip, in the direction where the tangential stress ($\sigma_{\theta\theta}$) is maximum.
2. propagation occurs when, in this direction, the quantity $\sigma_{\theta\theta}\sqrt{2\pi r}$ reaches a critical value K_{Ic} .

Practically, using the following expressions for the stresses around the crack tip in terms of polar coordinates:

$$\sigma_{\theta\theta} = \frac{1}{\sqrt{2\pi r}} \cos \frac{\theta}{2} \left[K_I \cos^2 \frac{\theta}{2} - \frac{3}{2} K_{II} \sin \theta \right] \quad (2)$$

$$\tau_{r\theta} = \frac{1}{\sqrt{2\pi r}} \frac{1}{2} \cos \frac{\theta}{2} \left[K_I \sin \theta + K_{II} (3 \cos \theta - 1) \right] \quad (3)$$

$$\sigma_{rr} = \frac{1}{\sqrt{2\pi r}} \cos \frac{\theta}{2} \left[K_I \left(1 + \sin^2 \frac{\theta}{2} \right) + \frac{3}{2} K_{II} \left(\sin \theta - 2 \tan \frac{\theta}{2} \right) \right] \quad (4)$$

the direction where $\sigma_{\theta\theta}$ is maximum by solving this system of an equation and inequality:

$$\frac{\partial \sigma_{\theta\theta}}{\partial \theta} = 0 \quad (5)$$

$$\frac{\partial^2 \sigma_{\theta\theta}}{\partial \theta^2} < 0 \quad (6)$$

The solution is represented in Fig. 4.

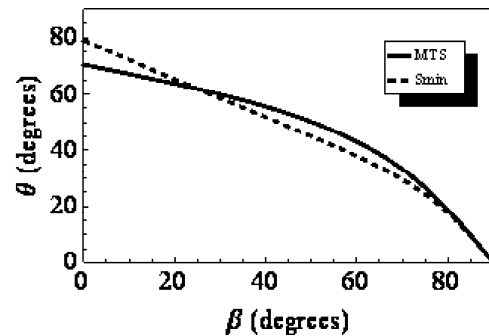


Figure 4. θ_0 vs. β curve following the MTS and the S_{min} criteria.

Slika 4. Kriva θ_0 u zavisnosti od β prema MTS i S_{min} kriterijumima.

For a plate with an inclined central crack of length a oriented with an angle β from the loading axis yy , it is shown that the K_I and K_{II} values are obtained from:

$$K_I = \sigma_{yy} \sqrt{\pi a} \sin^2 \beta \quad (7)$$

$$K_{II} = \sigma_{yy} \sqrt{\pi a} \sin \beta \cos \beta \quad (8)$$

and as for $\beta = 90^\circ$ in Eq. (7) $K_I = K_{Ic} = \sigma_{yy} \sqrt{\pi a}$, it is easily deduced that:

$$\frac{K_I}{K_{Ic}} = \sin^2 \beta \quad (9)$$

$$\frac{K_{II}}{K_{Ic}} = \sin \beta \cos \beta \quad (10)$$

The corresponding intrinsic curve is given in Fig. 3. If this curve is extrapolated to $K_I = 0$, we can see that K_{IIc} should be about 0.86. But, actually, it cannot be practically measured with a CCT plate with $\beta = 0$.

Another criterion, also proposed by G.C. Sih, [4, 3], searches the minimum of the strain energy density factor (SEDF) around a crack subjected to a mixed mode loading. This strain energy density can be expressed by a polynomial form:

$$S = a_{11}K_I^2 + 2a_{12}K_IK_{II} + a_{22}K_{II}^2 \quad (11)$$

where S is called the strain energy density factor. The a_{ij} are given by:

$$a_{11} = \frac{1}{16\mu} [(1 + \cos \theta)(\kappa - \cos \theta)] \quad (12)$$

$$a_{12} = \frac{1}{16\mu} \sin \theta [2 \cos \theta - (\kappa - 1)] \quad (13)$$

$$a_{22} = \frac{1}{16\mu} [(\kappa + 1)(1 - \cos \theta) + (1 + \cos \theta)(3 \cos \theta - 1)] \quad (14)$$

where μ is the shear modulus and

$$\kappa = \frac{3 - \nu}{1 + \nu} \quad \text{for plane stress} \quad (15)$$

$$\kappa = 3 - 4\nu \quad \text{for plane strain} \quad (16)$$

where ν is the Poisson's ratio.

Therefore the criterion is:

(i) the direction of crack propagation is that where the SEDF S is minimum,

(ii) crack extension occurs when S reaches a critical value S_{cr} ,

(iii) the length of crack propagation r_0 is such that S_{cr}/r_0

It is easy to derivate Eq. (11) versus θ and solve the system:

$$\frac{\partial S}{\partial \theta} = 0 \quad (17)$$

$$\frac{\partial^2 S}{\partial \theta^2} > 0 \quad (18)$$

The resulting curve is shown in Fig. 4. It can be seen that there are some differences between the two solutions. Through experimentation, we will try to verify which theory is the more adequate. Another test of fit will be realised through finite elements computing.

EXPERIMENTS

Fracture experiments on plates with a central inclined crack are described in details in [2]. Nine plates are cut from an aluminium alloy 2017 A and larger plate of 4 mm thickness. The mechanical characteristics of the alloy is given in Table 1. In each plate, a hole has been drilled in the centre and two notches are cut symmetrically. Then the plate is submitted to a fatigue loading, so that two symmetrical fatigue cracks propagate from each notch. Then,

taking the end of the fatigue cracks as a reference, the plate is cut again, so that a plate with an inclined central crack at a defined angle is obtained. Geometrical characteristics of the plates are given in Table 2. The initial plate is shown in Fig. 5 and the final plate in Fig. 6. It just should be underlined that for the 10° plate, the width is reduced to 75 mm so that the global tensile stress is lower than the ultimate stress.

After that, the plates are loaded in tension until fracture or general yielding occurs. The fracture load is noticed. Taking into account the crack length (which is more or less the same for each plate) the stress intensity factors in mode I and in mode II are computed using Eqs. (7) and (8).

The crack bifurcation angle θ_0 is also measured.

Table 1. Mechanical characteristics of 2017 A aluminium alloy.
Tabela 1. Mehaničke karakteristike legure aluminijuma 2017 A.

Yield stress, (MPa)	Ultimate stress, (MPa)	Fracture strain, (%)
328	440	21

Table 2. Geometrical characteristics of the plates.

Tabela 2. Geometrijske karakteristike ploča.

Angle (°)	90	80	65	60	50	40	30	20	10
Width (mm)	150	150	150	150	150	150	150	150	75
Length (mm)	450	450	450	450	450	450	450	450	450

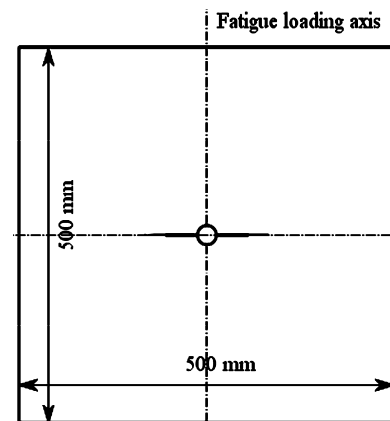


Figure 5. Initial plate with the hole, the notch and the fatigue crack.

Slika 5. Originalna ploča sa otvorom, zarezom i zamornom prslinom.

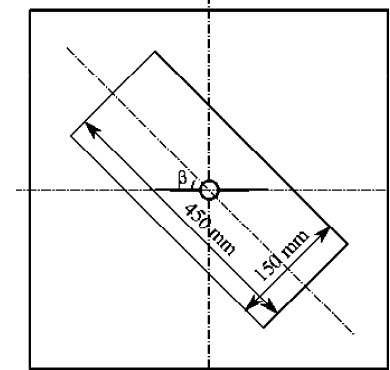


Figure 6. Cutting of the initial plate to obtain an inclined centre crack tensile specimen.

Slika 6. Šema rezanja originalne ploče radi dobijanja zatezne epruvete sa nagnutom središnjom prslinom.

EXPERIMENTAL RESULTS

The experimental results are given in Table 3 in terms of K_I and K_{II} and in terms of K_I/K_{Ic} and K_{II}/K_{Ic} , so that an intrinsic experimental curve can be built. A representation of these results is given on Fig. 7.

It can be seen that, if there is some concordance for high proportion of mode I, the experimental results diverge for low proportion of mode I.

Angles of bifurcation θ_0 are plotted versus the theoretical curves (Fig. 8). It can be seen that there is some agreement between the results and the S_{min} criterion.

Table 3. Experimental results for inclined centre crack tensile specimen.

Tabela 3. Eksperimentalni rezultati za zateznu epruvetu sa središnjom nagnutom prslinom.

β (°)	θ_0 (°)	K_I (MNm ^{-3/2})	K_{II} (MNm ^{-3/2})	K_I/K_{Ic}	K_{II}/K_{Ic}
90	0	59.1	0	1.00	0.00
80	12	53.8	8.5	0.91	0.14
65	29	53.5	22.3	0.91	0.38
60	36.5	46.0	25.9	0.78	0.44
50	47	41.1	33.0	0.70	0.56
40	62	29.4	33.5	0.50	0.57
30	67	19.9	32.9	0.34	0.56
20	75.5	11.2	28.4	0.19	0.48
10	81.5	5.9	15.1	0.10	0.26

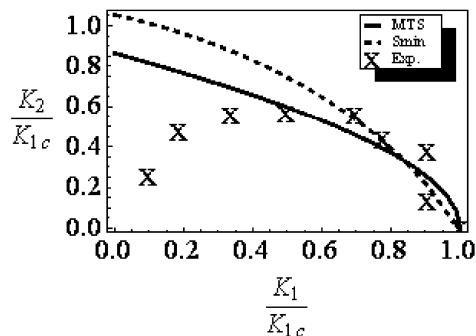


Figure 7. Experimental results and intrinsic curves following Maximum Tensile Stress and S_{min} criteria.

Slika 7. Eksperimentalni rezultati i unutrašnje krive prema kriterijumima Maksimalnog zateznog napona i S_{min} .

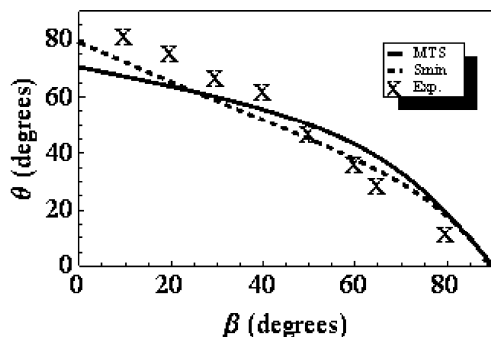


Figure 8. Experimental bifurcation angle versus MTS and S_{min} criteria.

Slika 8. Eksperimentalni bifurkacioni ugao prema kriterijumima MTS i S_{min} .

FINITE ELEMENTS COMPUTATIONS

To verify these results, finite element computations are realised using the Castem software.

The mesh is realised using triangular quadratic elements, with special Barsoum elements at the crack tip (Figs. 9 and 10), /5-6/. The computation is made using an elastic-plastic behaviour law with isotropic hardening, /7/. Computation of stress intensity factors both in mode I and II is made using the displacement of the crack lips.

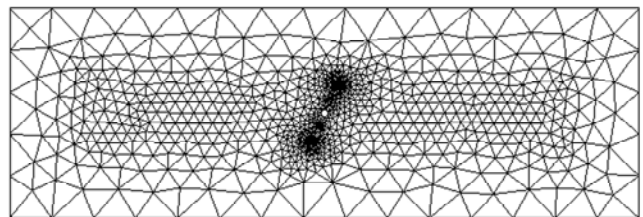


Figure 9. General mesh of a plate with a central inclined crack.
Slika 9. Opšta mreža elemenata za ploču sa središnjom nagnutom prslinom.

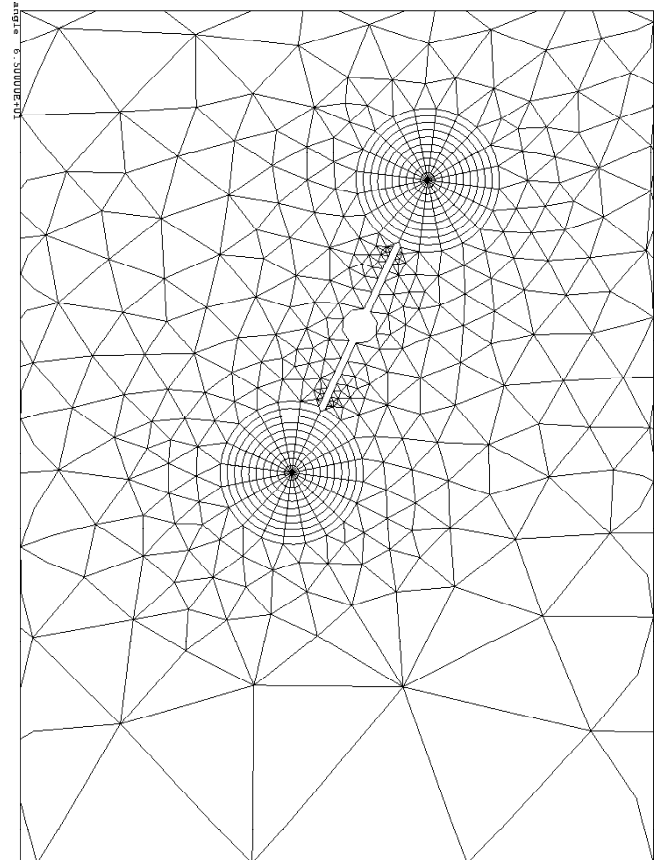


Figure 10. Detail of the cracked zone.
Slika 10. Detalj zone sa prslinom.

Results are shown in Fig. 11. It can be seen that some values seem completely out from the expected ones and very far from the experimental ones. This can be explained by the fact that, actually, yielding of the ligament area, then the general yielding of the plate occurs, and, therefore, the stress intensity factor is a nonsense. This is the reason why classical elastic theory diverges in some cases, particularly

when the ratio of mode I is low, corresponding logically with higher value of fracture load.

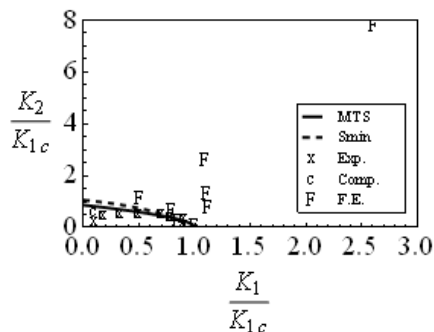


Figure 11. Comparison of experimental results, elastic and elastic-plastic computation.

Slika 11. Poređenje eksperimentalnih rezultata, elastični i elastoplastični proračun.

INTERPRETATION OF RESULTS

We have made two observations:

1. the fracture load
2. the bifurcation angle

The first one allows to compute the K_I and K_{II} stress intensity factors, using simple relationships or finite element computations using elastic or elastic-plastic behaviour laws. When the ratio of mode I is relatively high, the correspondence with the theoretical curve established with MTS or S_{min} criteria is relatively good, but they diverge drastically for low ratio of mode I. Simultaneously, the bifurcation angle experimentally measured gives a quite good agreement with the theoretical curves, whatever is the mode I ratio.

It is observed that the fracture load is determined on a load-displacement curve on an arbitrary point, probably the maximum load. It is suggested that this value approximately corresponds to the beginning of crack propagation, when the size of the plastic zone is relatively small with respect to the ligament size, but is much higher when the plastic zone size is large with respect to the ligament size. It probably corresponds to the general plastic collapse.

Conversely, the good agreement of crack propagation angle with the elastic theories is attributed to the fact that crack propagation initiates when the plasticity at crack tip is still limited, i.e. when elastic theories apply.

REFERENCES

1. Erdogan, F., Sih, G.C., *On the crack extension in plate under plane loading and transverse shear*, Journal of Basic Engineering - Trans ASME, 85: 519-527, 1963.
2. Jodin, Ph., *Contribution à l'étude des modes mixtes de rupture (mode I+II)*. Thèse d'état, Université de Metz, 1984.
3. Sih, G.C., *Strain energy density factor applied to mixed mode crack problems*, International Journal of Fracture, 10(3): 305-321, 1974.
4. Sih, G.C., *Three-Dimensional Crack Problems*, Volume Mechanics of Fracture II, chapter A Three-Dimensional Stress Energy Density Factor Theory of Crack Propagation, pages 15-53, Noordhoff International Publishing, Leyden, 1975.
5. Berković, M., *Determination of Stress Intensity Factors Using Finite Element Method*, Structural Integrity and Life, Vol.4, No2 (2004), pp.57-62.
6. Berković, M., *Numerical Methods in Fracture Mechanics*, Struct. Int. and Life, Vol.4, No2 (2004), pp.63-66.
7. Berković, M., Maksimović, S., Sedmak, A., *Analysis of Welded Joints by Applying the Finite Element Method*, Struct. Int. and Life, Vol.4, No2 (2004), pp.75-83.